

Relationship between the onset of ferromagnetism and the training effect in CMR perovskite manganites

This article has been downloaded from IOPscience. Please scroll down to see the full text article.

2004 J. Phys.: Condens. Matter 16 L101

(<http://iopscience.iop.org/0953-8984/16/8/L05>)

View [the table of contents for this issue](#), or go to the [journal homepage](#) for more

Download details:

IP Address: 129.252.86.83

The article was downloaded on 27/05/2010 at 12:45

Please note that [terms and conditions apply](#).

LETTER TO THE EDITOR

Relationship between the onset of ferromagnetism and the training effect in CMR perovskite manganites

D Zhu, V Hardy, A Maignan¹ and B Raveau

Laboratoire CRISMAT, UMR CNRS ENSICAEN 6508, 6 boulevard Maréchal Juin,
14050 Caen Cedex 4, France

E-mail: antoine.maignan@ismra.fr

Received 17 November 2003

Published 13 February 2004

Online at stacks.iop.org/JPhysCM/16/L101 (DOI: 10.1088/0953-8984/16/8/L05)

Abstract

Thermal cyclings in a zero field were shown to be able to significantly modify the magnetic properties of rare CMR mixed-valent manganites. The present letter reports on a precise investigation of this phenomenon (the so-called training effect) carried out on A-site substituted perovskite manganites, which allow a fine tuning of the magnetic ground state. Combining ac susceptibility and magnetization measurements during thermal cyclings, it is shown that the training effect is closely related to the transition from the orbital/charge ordered state to the ferromagnetic metallic state at low temperature, and consequently depends on T_C . We propose that this phenomenon originates from the structural phase separation that appears below T_C , in agreement with the martensitic-like scenario.

(Some figures in this article are in colour only in the electronic version)

Mixed-valent perovskite manganites have attracted considerable interest because they display a range of extraordinary properties including colossal magnetoresistance and charge ordering [1]. The half-doped manganite $\text{Pr}_{0.5}\text{Ca}_{0.5}\text{MnO}_3$ exhibits orbital and charge ordering (OO/CO) which corresponds to the 1:1 ratio of $\text{Mn}^{3+}:\text{Mn}^{4+}$ stripes and is a CE-type antiferromagnetic insulator (AFMI) [2]. This kind of AFMI state is very stable, therefore a high critical field up to 25 T is needed for melting it into a ferromagnetic (FM) state [3, 4]. If the Mn^{3+} content is increased (decreasing x from $x = 0.5$ in $\text{Pr}_{1-x}\text{Ca}_x\text{MnO}_3$), the OO/CO state is destabilized and the critical field decreases. $\text{Pr}_{0.6}\text{Ca}_{0.4}\text{MnO}_3$ with a pseudo CE-type AFM structure [5] exhibits a smaller critical field of about 8 T [3, 4, 6]. On the other hand, a decrease of critical field can be realized by substituting foreign cations either at the A- or B-site of the $\text{Pr}_{1-x}\text{Ca}_x\text{MnO}_3$ perovskite manganites ($0.5 \leq x \leq 0.6$) [7–10]. The substitution can lead to the development of FM in the AFM matrix, inducing phase separation (PS) [11–13]. In these

¹ Author to whom any correspondence should be addressed.

materials, by magnetic-field-driven magnetization ($M(H)$) measurements, we have found that the AFM to FM transition shows abrupt M steps at low temperature [7–10]. These features are not compatible with conventional metamagnetism, while a martensitic-like mechanism was found to be a plausible interpretation [14, 15]. This interpretation was proposed on the basis of several observations such as the training effect [9], influence of the measuring procedure [14], recovery of the virgin properties after annealing [16], role of the microstructure, etc [14–16].

The existence of PS can lead to very peculiar behaviours such as the effect of thermal cycling, which can induce a spectacular increase of resistivity and a change in the $M(H)$ shape [9, 17, 18]. Below the critical field H_1 for the appearance of the first $M(H)$ step, M shifts down and H_1 shifts up as the cycle number increases. This indicates that the FM regions tend to disappear to the benefit of the OO/CO AFM ones, as if the thermal cycling was a ‘training’ effect for the stabilization of the AFM phase.

In the recently studied $\text{Pr}_{1-x}(\text{Ca/Ba or Sr})_x\text{MnO}_3$ series, an unusually large training effect has been observed [10]. In order to understand the origin of this phenomenon, and especially the influence of T_C and of T_{CO} upon the training effect, we have revisited this system combining ac susceptibility measurements ($\chi(T)$) and low temperature isothermal $M(H)$ measurements. Two samples were selected, $\text{Pr}_{0.6}\text{Ca}_{0.38}\text{Ba}_{0.02}\text{MnO}_3$ and $\text{Pr}_{0.6}\text{Ca}_{0.34}\text{Sr}_{0.06}\text{MnO}_3$ which both exhibit a rather similar T_{CO} (204 and 217 K respectively), but differ in their T_C values (125 and 190 K respectively). We show that the training effect appears only below T_C . We discuss this behaviour within the framework of the martensitic mechanism, bearing in mind that the phase separation which takes place at low temperature is both electronic and structural [11–13].

Polycrystalline samples were prepared according to the experimental procedure previously reported [10]. $\chi'(T)$ and $M(H)$ were measured with a Quantum Design PPMS. Firstly, the sample was introduced into the chamber at a temperature of 300 K, secondly, it was cooled down to a limit temperature (T_{limit}), thirdly, it was warmed from T_{limit} up to 300 K, and finally it was cooled down to 2.5 K. In the above process, the temperature was swept at 1 K min^{-1} and $\chi'(T)$ was continuously measured using an excitation field and a frequency of 3 Oe and 10^3 Hz . Note that no static magnetic field was applied during either the cooling or warming process. The low ac magnetic field (3 Oe) does not affect the magnetic state. In the absence of a frequency effect (at least in the range $1\text{--}10^4 \text{ Hz}$) on the features of the training effect, the frequency $f = 1 \text{ kHz}$ of the ac magnetic field was chosen to optimize both duration and accuracy of the χ' measurements. After the completeness of this process, the $M(H)$ curve at 2.5 K was registered from 0 to 5 T and then from 5 to 0 T. For each magnetic field value, the magnetic field was settled with a sweep rate of 50 Oe s^{-1} and a 60 s pause was made prior to the magnetic moment collection.

The $\chi'(T)$ measurements performed upon cooling from 300 K down to $T_{\text{limit}} = 2.5 \text{ K}$ (the first curve) and then warming up to 300 K (the second curve) are shown for $\text{Pr}_{0.6}\text{Ca}_{0.38}\text{Ba}_{0.02}\text{MnO}_3$ in figure 1(a), and the inset is the enlargement of its $T_{\text{OO/CO}}$ region. The $\chi'(T)$ curve is characterized by two hysteretic temperature regions. The first one, extending from 125 K to $T_{\text{OO/CO}}$, reflects the structural transition from the disordered paramagnetic state above $T_{\text{OO/CO}}$ to the OO/CO paramagnetic state below $T_{\text{OO/CO}}$. The second one, between 30 and 125 K, is connected to a structural transformation from the distorted OO/CO phase to the less distorted weak FM phase [9]. The setting of the weak FM state can also be inferred from the $\chi''(T)$ curve (inset of figure 1(b)) where the existence of dissipation ($\chi'' > 0$) yields $T_C = 125 \text{ K}$. Another feature of the $\chi'(T)$ curves is the appearance of a cusp around 37 K for the cooling branch, suggesting that a spin glass-like behaviour is induced by Ba substitution [8, 10]. But, in contrast to typical spin-glasses, on the warming branch, the χ' maximum shifts up to 54 K. This irreversible

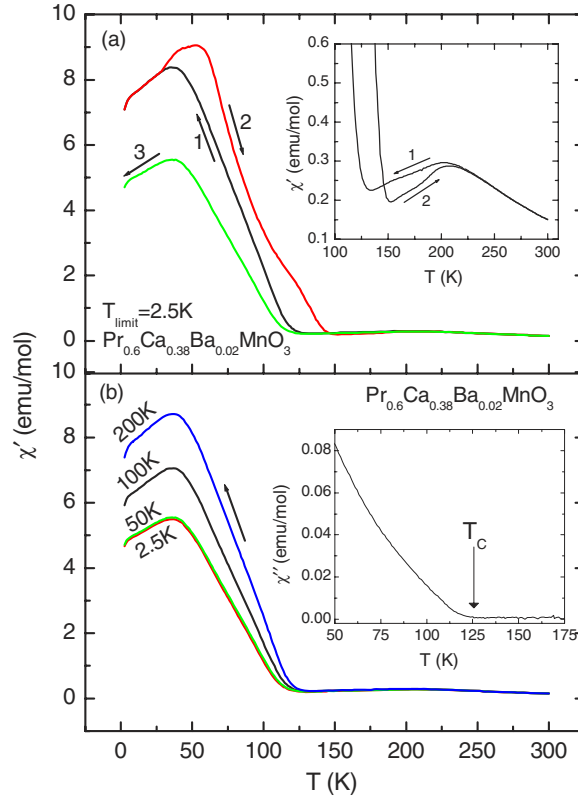


Figure 1. Real part of the ac magnetic susceptibility (χ') as a function of temperature for $\text{Pr}_{0.6}\text{Ca}_{0.38}\text{Ba}_{0.02}\text{MnO}_3$ collected upon cooling from 300 K to T_{limit} (curve 1), warming up from T_{limit} to 300 K (curve 2) and cooling again from 300 to 2.5 K (curve 3). (a) All three curves for $T_{\text{limit}} = 2.5$ K. Inset: the enlargement of the $T_{\text{OO/CO}}$ region for curves 1 and 2 with $T_{\text{limit}} = 2.5$ K. (b) The three curves for different T_{limit} , and the corresponding T_{limit} are labelled in the figure. Inset: T dependent imaginary part of the ac magnetic susceptibility (χ'') collected upon cooling a virgin sample showing the Curie temperature T_C .

behaviour is most probably associated with the second structural transformation. Similar characteristics are observed in the $\chi'(T)$ measurement of $\text{Pr}_{0.6}\text{Ca}_{0.34}\text{Sr}_{0.06}\text{MnO}_3$ as shown in the inset of figure 2, but its T_C is 190 K, which is much higher than that of the Ba-substituted sample. This difference is due to the larger A-site mismatch of the Ba-substituted sample compared to that of the Sr-substituted sample. Here, the effect of size mismatch on T_C [19] is predominant over that of the size of A-site cations. If we cool the above two samples down to 2.5 K and measure their $\chi'(T)$ again (the third curve), it is found that their third $\chi'(T)$ curves below T_C shift down dramatically compared to their first $\chi'(T)$ curves (figure 1(a) and inset of figure 2). This means that thermal cycling can stabilize the AFM state at the expense of the weak FM one. The same conclusion can be drawn from the measurement of $M(H)$ at 2.5 K. The M values below H_1 for the second $M(H)$ loop (300 \rightarrow 2.5 \rightarrow 300 \rightarrow 2.5 K) shift severely down in comparison with the first one (300 \rightarrow 2.5 K) for $\text{Pr}_{0.6}\text{Ca}_{0.38}\text{Ba}_{0.02}\text{MnO}_3$ (figure 3) and $\text{Pr}_{0.6}\text{Ca}_{0.34}\text{Sr}_{0.06}\text{MnO}_3$ (figure 4). On the other hand, it is obvious from figure 4(a) that H_1 shifts up as the number of cycles increases due to the training effect.

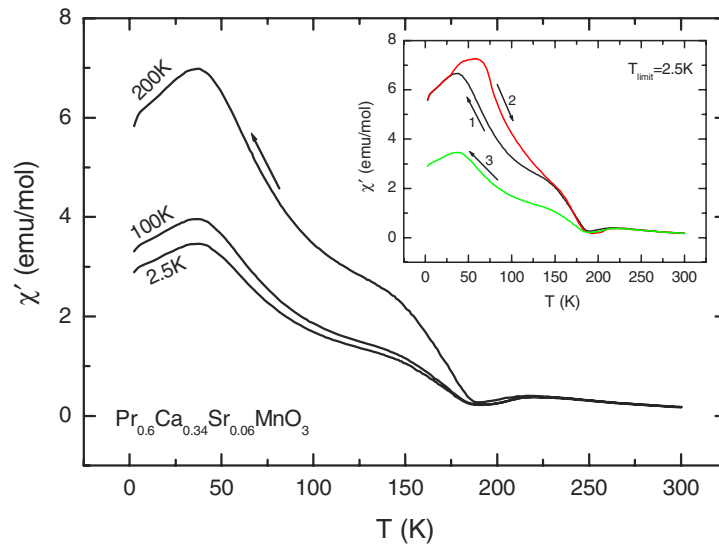


Figure 2. Real part of the ac susceptibility (χ') as a function of temperature for $\text{Pr}_{0.6}\text{Ca}_{0.34}\text{Sr}_{0.06}\text{MnO}_3$ collected upon cooling from 300 K to T_{limit} (curve 1), warming up from T_{limit} to 300 K (curve 2) and cooling again from 300 to 2.5 K (curve 3). The main panel shows the three curves for different T_{limit} , and the corresponding T_{limit} are labelled in the figure. Inset: all three curves for $T_{\text{limit}} = 2.5$ K.

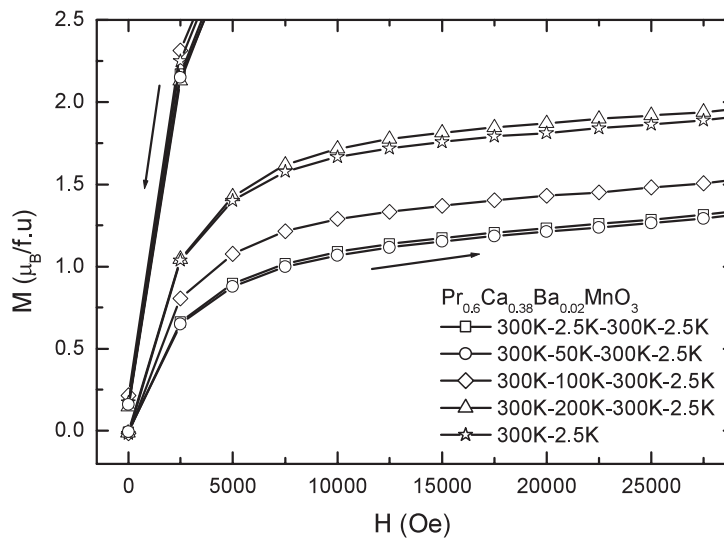


Figure 3. The enlargement of the field increasing branches of the isothermal $M(H)$ curves of $\text{Pr}_{0.6}\text{Ca}_{0.38}\text{Ba}_{0.02}\text{MnO}_3$ registered at $T = 2.5$ K after different thermal cyclings. The arrows indicate the magnetic field increasing and decreasing branches.

In order to determine what factor may induce the training effect, different limit temperatures were selected, as described in the experimental part. The cycling stages are labelled as numbers, i.e. 1 from 300 K to T_{limit} , 2 from T_{limit} to 300 K, 3 from 300 to 2.5 K, and then a $M(H)_{2.5\text{K}}$ half-loop is collected.

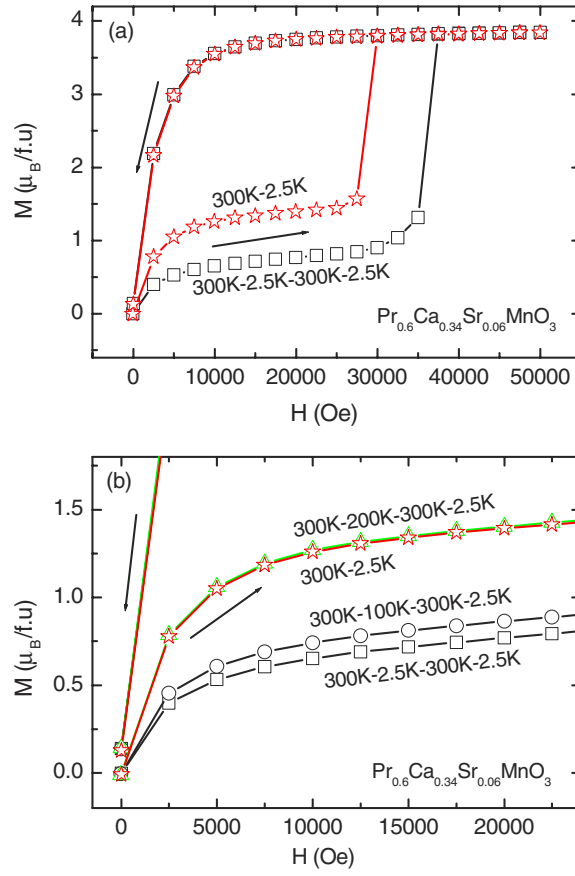


Figure 4. (a) Isothermal $M(H)$ curves of $\text{Pr}_{0.6}\text{Ca}_{0.34}\text{Sr}_{0.06}\text{MnO}_3$ registered at $T = 2.5$ K after different thermal cyclings (300 K–2.5 K and 300 K–2.5 K–300 K–2.5 K). (b) The enlargement of the field increasing branches of the $M(H)$ curves after different thermal cyclings. The arrows indicate the magnetic field increasing and decreasing branches.

Considering first $\text{Pr}_{0.6}\text{Ca}_{0.34}\text{Sr}_{0.06}\text{MnO}_3$, after complete cycling (1 \rightarrow 2 \rightarrow 3) with $T_{\text{limit}} = 200$ K one observes that the $\chi'(T)$ curve (figure 2) is very similar to the one corresponding to a single cooling from 300 to 2.5 K (figure 2). Similarly, the $M(H)$ curve with the same cycling procedure and with $T_{\text{limit}} = 200$ K (figure 4(b)) is practically superimposed on the curve without cycling, cooling directly the sample from 300 to 2.5 K. These results show that for a T_{limit} of 200 K, being between T_C (190 K) and T_{CO} (230 K), no training effect is induced in the sample. In contrast, for $T_{\text{limit}} = 100$ K, the $\chi'(T)$ curve after complete cycling (1 \rightarrow 2 \rightarrow 3) is very different from the one without cycling, as shown from figure 2. It is in fact very similar to the one obtained after complete cycling (1 \rightarrow 2 \rightarrow 3) for $T_{\text{limit}} = 2.5$ K (figure 2). In the same way, the $M(H)$ curve after complete cycling (1 \rightarrow 2 \rightarrow 3) with $T_{\text{limit}} = 100$ K, is very close to the one after complete cycling (1 \rightarrow 2 \rightarrow 3) with $T_{\text{limit}} = 2.5$ K (figure 4(b)), and much lower in magnetization than the one with direct cooling of the sample from 300 to 2.5 K (step 1 with $T_{\text{limit}} = 2.5$ K in figure 4(a)). Thus, a dramatic training effect is achieved in this Sr-substituted sample for T_{limit} values (2.5 and 100 K) smaller than T_C . This effect affects directly the ferromagnetic fraction at low temperature as shown as one compares the $\chi'(T = 2.5$ K) values from the inset of figure 2, called χ'_0 , obtained after the initial cooling

(or a cooling at $T_{\text{limit}} = 200$ K), $\chi'_0 = 5.8$ emu mol⁻¹, to the value $\chi'_0 = 2.9$ emu mol⁻¹ obtained after a cooling with $T_{\text{limit}} = 2.5$ K. A similar decrease by a factor of about two is also found by comparing the corresponding $M_{2.5\text{K}}(H = 2.5$ kOe) values (figure 4(b)). Such a low magnetic field (2.5 kOe) was previously used to determine the ferromagnetic fractions in similar compounds [7–10]. The same factor of two, coming from χ' and M values, shows that the initial ferromagnetic fraction at 2.5 K can be divided by two between the first cooling and a second cooling below T_C .

The above results suggest that the training effect only appears below T_C , and requires a transition from an AFM OO/CO state to FM state, but does not depend on the T_{CO} value. This viewpoint is confirmed by the study of $\text{Pr}_{0.6}\text{Ca}_{0.38}\text{Ba}_{0.02}\text{MnO}_3$, which exhibits a much lower T_C (125 K) and a similar T_{CO} (204 K). For $T_{\text{limit}} = 200$ K, i.e. much larger than T_C , no training effect is observed; after complete cycling at $T_{\text{limit}} = 200$ K ($1 \rightarrow 2 \rightarrow 3$) the $M(H)$ curve is practically superimposed on the curve obtained by direct cooling from 300 to 2.5 K (figure 3). The same behaviour is observed for the corresponding $\chi'(T)$ curves (figure 1). In contrast, after cycling ($1 \rightarrow 2 \rightarrow 3$) with $T_{\text{limit}} = 100$ K, the $M(H)$ curve is shifted down to lower M values compared to the direct cooling from 300 to 2.5 K (figure 3). The $M(H)$ curve after cycling with $T_{\text{limit}} = 2.5$ K is also shifted towards lower magnetization values with respect to the direct cooling from 300 to 2.5 K, but more importantly this curve exhibits significantly lower magnetization values than the one after cycling with $T_{\text{limit}} = 100$ K (figure 3). This difference is explained by the fact that the cycling close to T_C , i.e. at 100 K, is less efficient than at low temperature ($T_{\text{limit}} = 2.5$ K). This effect of the proximity of T_C is corroborated by the curve after cycling with $T_{\text{limit}} = 50$ K, which is practically superimposed on the one after cycling with $T_{\text{limit}} = 2.5$ K, both T_{limit} values being far from T_C . This effect of the T_{limit} value upon training is also clearly seen on the $\chi'(T)$ curves (figure 1(b)) which are superimposed for T_{limit} of 50 and 2.5 K, and exhibit smaller χ' values than for $T_{\text{limit}} = 100$ K after cycling ($1 \rightarrow 2 \rightarrow 3$).

These observations demonstrate that the appearance of the training effect in manganites requires the existence of a transition from an AFM OO/CO state to an FM. The absence of the effect for $T_{\text{limit}} > T_C$ suggests that it takes place below T_C . Bearing in mind that the AFM OO/CO to FM transition coincides with a structural transition from a more distorted to a less distorted phase, this behaviour can be understood on the basis of the phase separation scenario [11–13]. As soon as the temperature is lowered for the first time from 300 K to a temperature lower than T_C (e.g. 2.5 K), phase separation appears below T_C . The latter is both electronic and structural, i.e. it corresponds to the coexistence, below T_C , of the less distorted FM metallic phase with the more distorted AFM charge-ordered phase. Interfacial strains between the two structures are developed according to the martensitic-like mechanism previously proposed to explain the magnetization jumps [14, 15]. Since there is no phase separation for $T_{\text{limit}} > T_C$, the corresponding thermal cycling does not create interfacial strains so that no training effect is observed. In contrast, when the thermal cycling crosses T_C , by scanning the temperature from beyond T_C (this study) or from below T_C [18], the generated interfacial stresses can be sensitive to the thermal history of the sample. Nonetheless, it should be emphasized that there exist some compositions for which, despite a phase separated background state, the thermal cycling through T_C induces no change on the $\chi(T)$ curves [9]. The existence of these interfacial regions is thus necessary but not sufficient to observe a training effect.

In conclusion, this study shows the crucial role of the transition from the AFM OO/CO to the FM state, and especially of the coherent structural phase separation that appears below T_C , on the appearance of the training effect in manganites. It suggests that the interfacial strains between the two AFM OO/CO and FM phases are at the origin of the effect.

Dr Zhu would like to thank the French Ministry of Research for its support.

References

- [1] Rao C N R and Raveau B (ed) 1998 *Colossal Magnetoresistance, Charge Ordering and Related Properties of Manganese Oxides* (Singapore: World Scientific)
- Tokura Y (ed) 1999 *Colossal Magnetoresistance Oxides* (London: Gordon and Breach)
- [2] Goodenough J B 1995 *Phys. Rev.* **100** 564
- [3] Tokunaga M, Miura N, Tomioka Y and Tokura Y 1998 *Phys. Rev. B* **57** 5259
- [4] Respaud M, Llobet A, Frontera C, Ritter C, Broto J M, Rakoto H, Goiran M and García-Muñoz J L 2000 *Phys. Rev. B* **61** 9014
- [5] Jirak Z, Krupicka S, Simsa Z, Dlouha M and Vratislav S 1985 *J. Magn. Magn. Mater.* **53** 153
- [6] Tomioka Y, Asamitsu A, Kawahara H, Moritono Y and Tokura Y 1996 *Phys. Rev. B* **53** R1698
- [7] Hébert S, Maignan A, Martin C and Raveau B 2002 *Solid State Commun.* **121** 229
- [8] Hébert S, Maignan A, Hardy V, Martin C, Hervieu M and Raveau B 2002 *Solid State Commun.* **122** 335
- [9] Maignan A, Hébert S, Hardy V, Martin C, Hervieu M and Raveau B 2002 *J. Phys.: Condens. Matter* **14** 11809
- [10] Raveau B, Zhu D, Maignan A, Hervieu M, Martin C, Hardy V and Hébert S 2003 *J. Phys.: Condens. Matter* **15** 7055
- [11] Kimura T, Tomioka Y, Kumai R, Okimoto Y and Tokura Y 1999 *Phys. Rev. Lett.* **83** 3940
- [12] Moreo A, Yunoki S and Dagotto E 1999 *Science* **283** 2034
- [13] Uehara M, Mori S, Chen C H and Cheong S-W 1999 *Nature* **399** 560
- [14] Hardy V, Hébert S, Maignan A, Martin C, Hervieu M and Raveau B 2003 *J. Magn. Magn. Mater.* **264** 183
- [15] Podzorov V, Kim B G, Kiryukhin V, Gershenson M E and Cheong S-W 2001 *Phys. Rev. B* **64** 140406
- [16] Hardy V, Yaicle C, Hébert S, Maignan A, Martin C, Hervieu M and Raveau B 2003 *J. Appl. Phys.* **94** 5316
- [17] Mahendiran R, Raveau B, Hervieu M, Michel C and Maignan A 2001 *Phys. Rev. B* **64** 064424
- [18] Maignan A, Hardy V, Martin C, Hébert S and Raveau B 2003 *J. Appl. Phys.* **93** 7361
- [19] Rodriguez-Martinez L M and Attfield J P 1998 *Phys. Rev. B* **58** 2426